Conference on Modelling Fluid Flow (CMFF'25)
The 19th International Conference on Fluid Flow Technologies
Budapest, Hungary, August 26 - August 29, 2025

ENHANCING PREDICTIVE ACCURACY OF TURBULENT SUBCOOLED FLOW BOILING USING LES

Hanan ABUREMA[1], Bruce C HANSON[2], Michael FAIRWEATHER[3], Marco COLOMBO[4]

[1] Corresponding Author. School of Chemical & Process Engineering, University of Leeds, Leeds LS2 9JT, UK. E-mail: pmhaa@leeds.ac.uk
[2] School of Chemical & Process Engineering, University of Leeds, Leeds LS2 9JT, UK. E-mail: b.c.hanson@leeds.ac.uk
[3] School of Chemical & Process Engineering, University of Leeds, Leeds LS2 9JT, UK. E-mail: m.fairweather@leeds.ac.uk
[4] School of Mechanical, Aerospace & Civil Engineering, University of Sheffield, Sheffield S10 2TN, UK. E-mail: m.colombo@sheffield.ac.uk

ABSTRACT

The high heat transfer rates required in many cooling systems can often only be achieved through subcooled boiling flows in heated wall regions, with boiling providing the heat transfer rates required to maintain system integrity. Understanding the mechanism of boiling in systems with turbulent subcooled flows is essential for enhancing the predictive capabilities for nuclear thermal hydraulic systems. This study investigates two boiling models coupled with large eddy simulations employing a dynamic subgrid-scale eddy viscosity model. One boiling model utilises a mechanistic force balance approach to predict bubble dynamics: accounting for the bubble growth and detachment processes affected by micro-layer evaporation, heat transfer from the superheated liquid, and condensation on the bubble cap due to the subcooled liquid. The other model employs a reduced correlation-based approach to determine bubble departure diameter and frequency, aiming to improve the applicability of the force balance method while reducing computational and calibration requirements. To evaluate the performance of these models, validation is conducted against experimental data for vertically upward subcooled boiling flows using water and refrigerant R12. These datasets encompass a wide range of operating conditions, ensuring a robust and comprehensive assessment of model accuracy. Results indicate that both models achieve satisfactory predictive accuracy across all tested conditions, demonstrating improvements over equivalent Reynolds-Averaged Navier-Stokes-based approaches. Although the mechanistic model provides superior precision in predicting bubble dynamics, this enhanced accuracy comes at the cost of increased computational demand, making the correlation-based approach a viable alternative for engineering applications requiring reduced computational expense. These findings contribute to the ongoing development of high-fidelity boiling models for nuclear thermal hydraulic simulations, offering valuable insights for future research and industrial applications.

Keywords: subcooled boiling, bubble dynamics, large eddy simulation, force balance model, reduced correlation

NOMENCLATURE

F_b	$[N]$	buoyancy force
F_{cp}	$[N]$	contact pressure force
F_{du}	$[N]$	unsteady drag force
F_p	$[N]$	hydrodynamic force
F_{st}	$[N]$	surface tension force
G_s	[-]	dimensionless shear rate
Ja	[-]	Jacob number
P	$[Pa]$	pressure
R	$[m]$	bubble radius
S	$[1/s]$	rate of strain tensor
d_B	$[m]$	bubble diameter
d_{dep}	$[m]$	bubble departure diameter
d_w	$[m]$	contact diameter
g	$[m/s^2]$	gravitational acceleration
t	$[s]$	time
u	$[m/s]$	velocity
u_τ	$[m/s]$	shear velocity
u^+	[-]	dimensionless velocity
y^+	[-]	dimensionless wall distance
Γ	$[kg/m^3.s]$	mass transfer rate
Δ	$[m]$	filtering width
α	[-]	void fraction
μ	$[kg/m\ .s]$	dynamic viscosity
ν	$[m^2/s]$	kinematic viscosity
ρ	$[kg/m^3]$	density

Subscripts and Superscripts

G	gas
I	Either phase
L	liquid
d	drag
x, *y*	spatial coordinates

1. INTRODUCTION

Boiling phenomena in turbulent subcooled flows are crucial for achieving efficient heat transfer, particularly in thermal hydraulic systems, making it a key focus for researchers in both industry and academia. Subcooled flow boiling plays a critical role in applications requiring effective cooling, such as nuclear reactors, refrigeration systems, and in the chemical processing industries [1]. However, this process is highly complex due to the intricate dynamics of bubble nucleation, growth, detachment, and dispersion near heated surfaces. A comprehensive understanding of these phenomena is crucial for optimising system designs, enhancing performance, and ensuring the reliability and safety of advanced thermal systems.

The transient and complex nature of boiling phenomena makes it difficult to fully understand their underlying physical mechanisms. Experimental studies have primarily aimed at developing empirical correlations based on extensive datasets obtained under diverse geometries, fluid types, and operating conditions [2, 3]. However, these experiments are expensive, and the resulting correlations are often limited to the specific conditions and setups used. To overcome these limitations, computational fluid dynamics (CFD), and particularly Eulerian-Eulerian approaches, have been widely employed to model flow boiling, providing a more adaptable and cost-effective tool for investigating these processes [4].

In this approach, the conservation equations for mass, momentum, and energy are solved separately for each phase. However, this method simplifies the system by averaging the phase occurrence over time and space, which results in the loss of detailed interface structure information. As a result, additional models are required to account for the exchange of mass, momentum, and energy between the phases [5]. The phase change at the heated wall and the distribution of heat flux between the liquid and vapour phases are typically modelled using wall boiling models. One of the most widely used heat flux partitioning models is the Rensselaer Polytechnic Institute (RPI) model [6], in which the external heat flux applied to the heating wall is divided into three primary heat transfer mechanisms: single-phase convection, quenching, and evaporation. These mechanisms depend on several key parameters, including nucleation site density, bubble departure diameter, and bubble departure frequency, with correlations for these quantities initially derived from pool boiling experiments conducted at ambient pressure [7]. A detailed review of the available correlations can be found in [8]. Numerous studies have evaluated the applicability of the RPI model using the standard correlations implemented in most CFD packages. However, these studies have shown that the model often exhibits limited accuracy and generality [4].

Among the key parameters requiring accurate modelling, the bubble departure diameter is particularly important for predicting the void fraction distribution within the flow. Consequently, mechanistic sub-models that explicitly describe bubble dynamics are essential for improving predictive accuracy. Klausner et al. [9] developed a mechanistic model based on a force balance during the bubble's growth phase prior to its departure from a surface. This model demonstrated good predictive performance against their experimental data. Over the years, many researchers have worked on improving the original model to increase its predictive capability across a wider range of experimental conditions [10]. One significant enhancement involved incorporating local condensation effects into the bubble growth rate model, along with modifications to the lift force and surface tension models [11]. Further improvements were made by integrating microlayer evaporation beneath the bubble to enhance model accuracy [12]. Recent research conducted at the Massachusetts Institute of Technology (MIT) has introduced a comprehensive approach to heat flux partitioning by incorporating all essential wall nucleation closures [13]. Using experimental data obtained through advanced measurement techniques, the MIT model provides wall nucleation closures that are applicable across a wide range of pressures and flow conditions. Unlike conventional models, this approach eliminates the need for case-specific calibration, improving its adaptability and reliability [14].

Most existing modelling efforts for subcooled boiling have relied on Reynolds-averaged Navier-Stokes (RANS) approaches due to their relatively low computational cost. However, RANS models tend to over-predict mixing and fail to capture the complex transient dynamics of turbulent flow boiling due to their inherent averaging of turbulent fluctuations. To address these limitations, researchers have increasingly turned to large eddy simulation (LES), which offers a more accurate and robust framework for studying complex boiling phenomena [15]. Although LES requires significantly greater computational resources than RANS-based approaches, continuous advancements in computing power are making it increasingly feasible for high-fidelity analysis and optimisation of boiling flows. In this study, the bubble dynamics model and the reduced-correlation MIT model are implemented in the OpenFOAM code and compared within an LES framework. LES allows a detailed investigation of subcooled boiling flows, offering

improved accuracy in capturing key phenomena. Both models are validated against experimental data for vertically upward boiling flows using water and refrigerant R12 over a wide range of conditions.

2. MATHEMATICAL MODELLING

By spatially filtering the governing equations in the Eulerian-Eulerian two-fluid model in LES, large-scale motions are explicitly resolved, while small subgrid-scale (SGS) fluctuations are modelled:

$$\frac{\partial(\alpha_I \rho_I)}{\partial t} + \nabla.(\alpha_I \rho_I u_I) = \Gamma \tag{1}$$

$$\frac{\partial(\alpha_I \rho_I u_I)}{\partial t} + \nabla.(\alpha_I \rho_I u_I u_I) = \alpha_I \rho_I g - \alpha_I \nabla P + \nabla.(\alpha_I \tau_I) + M_I \tag{2}$$

The influence of the unresolved scales on the resolved scales is represented through the SGS stress tensor, which is modelled as:

$$\tau_i = -\mu_{eff}\left((\nabla u_I) + (\nabla u_I)^T - \frac{2}{3} I(\nabla . u_I)\right) \tag{3}$$

For the liquid phase, the effective viscosity μ_{eff} is determined by considering molecular viscosity, turbulent viscosity, and bubble-induced turbulence, with the latter being modelled using the Sato et al. [16] model, ensuring an accurate representation of the flow dynamics:

$$\mu_{eff} = \mu_{L,L} + \mu_{T,L} + \mu_{BI,L} \tag{4}$$

$$\mu_{BI,L} = \rho_L C_{BI} \alpha_G d_B |u_G - u_L| \tag{5}$$

In this study, the dynamic Smagorinsky SGS model is used to model the unresolved turbulence viscosity, which relies on applying a second filter considering both spatial and temporal variations:

$$\mu_{T,L} = \rho_L (C_s \Delta)^2 \left|\overline{S_{ij}}\right| \tag{6}$$

The precision of the model is improved by accounting for such variations, making it more dependable for capturing flow dynamics. It employs a dynamic procedure to calculate C_s based on the resolved stress tensor L_{ij} and the Germano rate of strain tensor M_{ij} through an iterative process [17]:

$$C_s = \frac{1}{2}\frac{L_{IJ} M_{IJ}}{M_{IJ} M_{IJ}} \tag{7}$$

$$L_{IJ} = \widehat{\bar{u}_\iota \bar{u}_j} - \hat{\bar{u}}_\iota \hat{\bar{u}}_j \tag{8}$$

$$M_{IJ} = \Delta^2 \widehat{\bar{S}_{\iota j} \bar{S}_{\iota j}} - \hat{\bar{S}}_{\iota j} \hat{\bar{S}}_{\iota j} \tag{9}$$

The turbulence kinetic energy is modelled based on the dynamic procedure as:

$$k = C_s . \Delta^2 . |S|^2 \tag{10}$$

For the gas phase, turbulence is not resolved, and the effects of liquid-phase turbulence on the gas phase are neglected. This simplification reduces model complexity and avoids the need for additional equations to account for gas-phase turbulence. The interfacial momentum transfer term M_I introduces the dynamic interaction between the phases in a multiphase flow. This term primarily accounts for contributions from various forces, including drag, lift, wall lubrication, turbulent dispersion, virtual mass, surface tension, and phase change mass transfer forces, particularly in the context of boiling flow. The drag force is the resistance experienced by a bubble as it moves through the liquid, modelled as:

$$F_d = \frac{3}{4}\frac{C_d}{d_B} \alpha_G \rho_L |(u_G - u_L)|(u_G - u_L) \tag{11}$$

The drag coefficient C_d is calculated using the drag model proposed by Tomiyama et al. [18]. The bubbles moving in a shear flow experience a lift force perpendicular to their direction of motion, influencing the radial void distribution in pipes, with small bubbles pushed towards the wall, while larger bubbles tend to move toward the centre after reaching a critical diameter. The wall force, on the other hand, keeps bubbles away from the wall. However, due to the limited understanding of the contributions of lift and wall forces in boiling flows [4], these forces are neglected in this study. The virtual mass force is accounted for using a fixed coefficient of 0.5, and the turbulent dispersion force is modelled following Lopez de Bertodano [19], with a turbulent dispersion coefficient 0.7.

$$F_{vm} = \alpha_G \rho_L C_{vm}\left(\frac{Du_G}{Dt} - \frac{Du_L}{Dt}\right) \tag{12}$$

$$F_{td} = k \nabla \alpha_G \rho_L C_{td} \tag{13}$$

The multiple size group (MUSIG) population balance model is used, which is part of OpenFOAM, with bubble coalescence modelled according to [20] and break-up based on [21].

3. WALL BOILING MODEL

In the mechanistic approach to modelling boiling, the bubble departure diameter is determined by the bubble growth rate, which is predicted through an energy balance. This balance incorporates the heat transfer mechanisms between the bubble, the heated wall, and the surrounding liquid. Recently, Colombo and Fairweather [12] proposed a combined equation that integrates the contributions of superheating and subcooling in predicting the bubble growth rate during flow boiling. These phenomena are crucial as they influence the overall heat transfer efficiency of the system. During the growth process, the forces acting on the bubble can be classified into *x*-direction adhesive forces, which keep the bubble attached to

the nucleation site, and *y*-direction detaching forces which act to separate the bubble from the surface. When the resultant detaching forces exceed the adhesive forces, the bubble departs from the nucleation site. Similarly, for a sliding bubble, if the detaching forces surpass the adhesive forces, the bubble lifts off from the heated surface and moves toward the bulk flow. The various forces influencing bubble growth at the nucleation site are shown in Figure 1, which demonstrates these interactions, with the model summarised in Table 1.

Table 1. Summary of the closures used with the force balance model (FB)

Model	Form
Bubble departure diameter	Klausner et al [9] $\sum F_y = F_{sty} + F_{sl} + F_b \cos\theta + F_{duy} + F_p + F_{cp}$ $\sum F_x = F_{st} + F_{qsd} + F_b \sin\theta + F_{dux}$ $F_{stx} = -1.25 d_w \sigma \frac{\pi(\alpha-\beta)}{\pi^2-(\alpha-\beta)^2}(sin\alpha - sin\beta)$ $F_{sty} = -d_w \sigma \frac{\pi}{(\alpha-\beta)}(cos\beta - cos\alpha)$ $F_{qsd} = 6\pi\rho_l \nu U R \left\{\frac{2}{3} + \left[\left(\frac{12}{Re}\right)^{0.65} + 0.862\right]^{-1.54}\right\}$ $F_{du} = -\rho_l R^2 \left(\frac{2}{3}R^{\cdot 2} + RR^{\cdot 2}\right)$ $F_b = \frac{4}{3}\pi R^3(\rho_l - \rho_g)g$ $F_{sl} = \frac{1}{2}\pi\rho_l U R^2 \left\{3.877 G_s^{0.5}[Re^{-2} + (C_l G_s^{0.5})^4]^{\frac{1}{4}}\right\}$ $F_p = \frac{9}{8}\rho_l U^2 \frac{\pi d_w^2}{4}$ $F_{cp} = \frac{\sigma}{R}\frac{\pi d_w^2}{4}$ Yun et al. [11] $d_w/d_{dep} = 0.067,\ C_l = 0.118$
Bubble growth	Colombo and Fairweather [12] $\frac{dR(t)}{dt} = \frac{1}{C_2} Pr^{-0.5} Ja \left(\frac{k_l}{\rho_l C_{p,l}}\right)^{0.5} t^{-0.5} + \sqrt{\frac{3}{\pi}} Ja \left(\frac{k_l}{\rho_l C_{p,l}}\right)^{0.5} (1-b) t^{-0.5} - \frac{h_c}{\rho_l h_{lg}}(T_{sat} - T_{sub})b$
Nucleation site density	Hibiki and Ishii [22] $N_a` = N_0 \left[1 - exp\left(-\frac{\theta^2}{8\mu^2}\right)\right]\left[exp\left(f` \frac{\lambda`}{R_c}\right) - 1\right]$
Bubble departure frequency	Cole [23] $f = \sqrt{\frac{3}{4}\frac{g(\rho_l - \rho_g)}{d_w \rho_l}}$

In the MIT framework, the departure diameter refers to the bubble size at the moment it detaches from the nucleation site, either by sliding along the heated surface or by moving into the bulk liquid. In contrast, the lift-off diameter describes the size of a sliding bubble at the instant it detaches from the heated surface entirely and moves into the bulk flow. Another essential parameter in the MIT framework is the bubble departure frequency, which is determined by incorporating bubble wait time and an improved representation of bubble growth dynamics, derived from a force balance approach. This methodology captures the interplay between wall superheat and flow subcooling, enabling the accurate prediction of bubble behaviour and detachment trends under various boiling conditions.

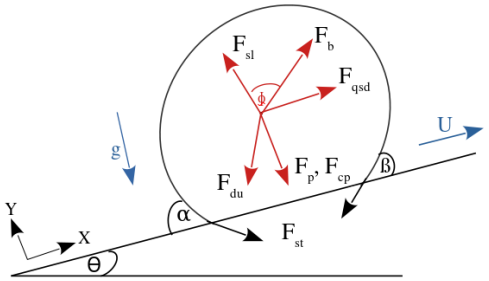

Figure 1. Forces acting on a bubble at the nucleation site

Table 2. Summary of the closures used with the MIT model

Model	Form
Bubble departure diameter	Kommajosyula [13] $18.6\ 10^{-6}\left(\frac{\Delta\rho}{\rho_g}\right)^{0.27} Ja_{sup}^{0.75}(1 + Ja_{sub})^{-0.3} u_l^{-0.26}$
Bubble growth	Kommajosyula [13] $K = \frac{\sqrt{k_l}}{0.804\sqrt{Pr}} Ja_{sup} + \mathcal{X} 1.95 Ja_{sup} k_l$
Nucleation site density	Lemmert and Chawla [24] $N_a = C_n N_{ref}\left(\frac{\Delta T}{dT_{ref}}\right)^{1.805}$
Bubble departure frequency	Kommajosyula [13] $f = \frac{1}{t_{growth}+t_{wait}}$ $t_{growth} = \left(\frac{d_{dep}}{4K}\right)^2$ $t_{wait} = \frac{0.0061\ Ja_{sub}^{0.63}}{\Delta T_{sup}}$

The MIT model represents a robust subcooled flow boiling formulation with new closures applicable over a wide range of flow conditions. In this study, two key closures have been tested: the bubble departure diameter and the bubble departure frequency. By evaluating these closures, the results contribute to a deeper understanding of bubble dynamics in boiling flows and enhance the predictive capabilities of the model. The model parameters and

closures used with the MIT framework are summarised in Table 2.

4. WALL TREATMENT

In LES, the accurate representation of the near-wall region is essential due to the significant velocity gradients near a surface. The standard logarithmic law often fails to capture the complexities of non-equilibrium wall functions and pressure gradient effects, especially in the presence of strong turbulence. To overcome these limitations, Spalding's formula [25] is used, where the turbulence length scale, y^+, is defined as follows:

$$y^+ = u^+ + \frac{1}{E}\left[e^{cu^+} - 1 - cu^+ - \frac{(cu^+)^2}{2} - \frac{(cu^+)^3}{6}\right] \quad (13)$$

where E = 9.025 and c = 0.4, and the dimensionless parameters y^+ and u^+ are defined as:

$$y^+ = \frac{yu_\tau}{\nu} \ , u^+ = \frac{u}{u_\tau} \quad (14)$$

Since Spalding's equation is nonlinear, an iterative procedure, such as the Newton-Raphson method, must be used to solve for u_τ .This method ensures rapid convergence and improves the accuracy of near-wall turbulence modelling by capturing velocity variations more effectively.

5. EXPERIMENTAL AND NUMERICAL SETUP

Two experiments were selected to validate the numerical simulations in this study: the DEBORA experiments [26], and the Bartolomei and Chanturiya [27] experiment. The DEBORA experiments investigated subcooled boiling of Freon-12 in a vertical pipe with an inner diameter of 19.2 mm and a length of 3.5 m, simulating high-pressure water boiling at pressures ranging from 1.46 to 3.01 MPa. In contrast, the Bartolomei and Chanturiya experiment examined subcooled boiling of water in a vertical pipe with a 15.4 mm inner diameter and a heated length of 2 m, operating at pressures up to 15 MPa. Both experiments provided critical data, including area-averaged void fractions, wall temperatures, average bubble diameters, and liquid temperatures. These datasets serve as reliable benchmarks for assessing computational fluid dynamic models as they effectively capture boiling conditions relevant to nuclear reactor systems while remaining experimentally accessible.

The numerical simulations were conducted using a three-dimensional axisymmetric geometry, with the computational domain designed to replicate the experimental setups. To reduce computational cost while maintaining accuracy, a 10° wedge of each pipe was employed as the computational domain. A fully developed velocity profile was specified at the inlet of the domain to ensure representative flow conditions, which is essential for capturing realistic flow behaviour. At the top outlet, a pressure boundary condition was imposed. For the liquid phase, a no-slip boundary condition was applied at the wall, while a free-slip condition was used for the vapour phase to account for the negligible shear stress at the wall for this phase. A central differencing scheme was used for the advection term to minimise numerical diffusion and enhance accuracy. For time discretisation, a second-order backward Euler scheme was selected to improve temporal accuracy and stability. These schemes were chosen to ensure a robust and accurate representation of the complex boiling phenomena under investigation. However, it is important to note that the computational cost varied significantly between the models. The simulation time using the mechanistic model was approximately twice that of the MIT model, primarily due to the detailed treatment of bubble dynamics, which requires additional computational resources to resolve small-scale boiling mechanisms accurately.

6. RESULTS AND DISCUSSION

The results demonstrate the performance of the LES framework when coupled with two distinct boiling models: a mechanistic force balance approach and the reduced, correlation-based MIT model. These models are validated using experimental data for vertically upward subcooled boiling flows. In addition, comparisons are made with previous studies [28] that employed a force balance approach while neglecting subcooling effects, obtained using a RANS-based method. The analysis focuses on key parameters, including void fraction distribution, average bubble diameter, and wall temperature profiles.

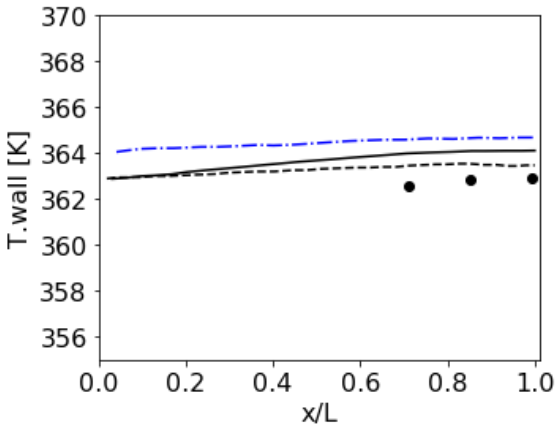

Figure 2. Wall temperature predictions along the heated wall for DEBORA experiment [26]: • data; — FB; --- MIT; - - - Colombo et al. [28]

In Figure 2, which compares predictions with the DEBORA experiment, both the force balance and MIT models tend to over-predict the wall

temperature, with RANS showing the highest over-predictions.

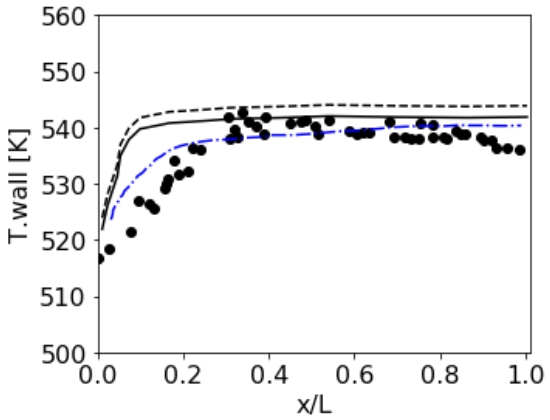

Figure 3. Wall temperature predictions along the heated wall for Bartolomei and Chanturiya experiment [27]: • data; — FB; --- MIT; - · - Colombo et al. [28]

More detailed experimental axial wall temperatures along the pipe length are available for the Bartolomei and Chanturiya [27] case, as shown in Figure 3. Here, the temperature exhibits a rapid increase in the early regions of the pipe, followed by a levelling off and a slight decline towards the outlet. Both the mechanistic and MIT models roughly follow the experimental trend, capturing the rise in wall temperature close to the pipe inlet, although the rate of increase is significantly over-estimated. This increase is primarily influenced by local flow acceleration and changes in heat transfer mechanisms.

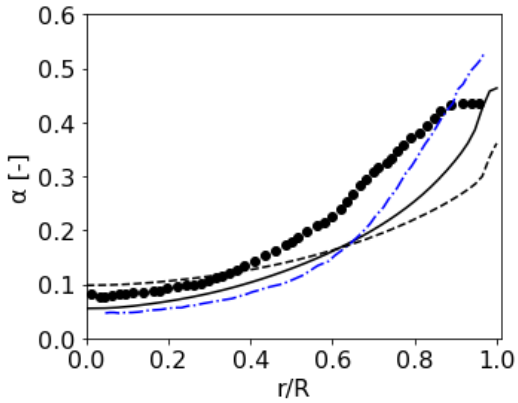

Figure 4. Radial void fraction predictions for DEBORA experiment [26]: • data; — FB; --- MIT; - · - Colombo et al. [28]

Once boiling begins, however, both models show good agreement with the experimental data. The mechanistic model slightly over-predicts the wall temperature, particularly near the pipe end, although less so that the MIT model, most likely due to its detailed treatment of bubble dynamics and heat flux partitioning. Over-prediction by the MIT model can be attributed to its simplified correlation-based approach which does not fully capture the intricate interactions between bubble dynamics and heat transfer, especially under subcooled boiling conditions. In contrast, the predictions from Colombo et al. [28], which rely on a RANS-based approach, show a significant over-prediction of wall temperature for the DEBORA experiment (Figure 2). This discrepancy may stem from the limitations of the RANS framework in resolving complex heat transfer mechanisms and bubble dynamics, particularly in regions where subcooling and phase interactions play a critical role. When comparing similar predictions with the data from Bartolomei and Chanturiya [27], the RANS-based approach, as presented by Colombo et al. [28], shows good agreement with the experimental data in the boiling region but also exhibits a slight overprediction in the non-boiling region.

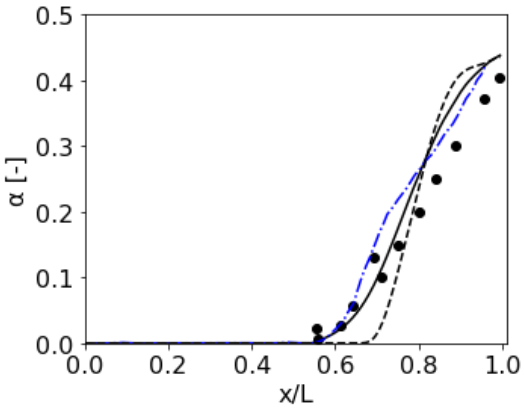

Figure 5. Radial void fraction predictions for Bartolomei and Chanturiya experiment [27]: • data; — FB; --- MIT; - · - Colombo et al. [28]

The predicted radial void fraction profiles, shown in Figures 4 and 5, reveal a wall-peaked distribution, consistent with experimental observations. For the DEBORA experiment, the mechanistic model captures this trend with good agreement to the experimental data, though it slightly over-predicts the void fraction near the wall, similar to the predictions from Colombo et al [28]. This over-prediction highlights the model's detailed resolution of bubble nucleation, growth, and detachment processes. A larger predicted bubble departure diameter results in longer residence times before detachment, leading to a higher evaporative heat flux at the wall. Conversely, smaller bubble departure diameter reduces the evaporative heat flux, causing an increase in wall temperature to maintain a constant flux. The resulting rise in wall temperature may enhance nucleation site density, subsequently increasing the void fraction. In contrast, the MIT model also predicts a wall-peaked profile but shows a lower void fraction near the wall compared to the experimental data. This discrepancy can be attributed to the model's assumption of extended bubble

attachment times, which increases the duration of bubble growth and reduces the frequency of bubble detachment. As a result, fewer bubbles are released into the flow, leading to a lower overall void fraction near the wall. For the Bartolomei and Chanturiya [27] experiment, all the models show a reasonable agreement with the data in Figure 5, although the force balance approach is generally superior. The MIT model indicates later onset boiling, occurring after the pipe's midpoint. This delayed transition to boiling corresponds to the higher predicted wall temperatures (Figure 3), which result from a decreasing local evaporation heat flux at the wall. As more heat is absorbed by the liquid phase prior to bubble lift-off, wall temperatures rise accordingly.

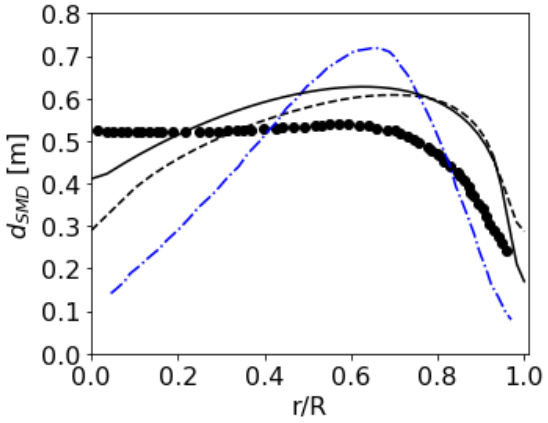

Figure 6. Radial averaged mean diameter predictions for DEBORA experiment [28]: • data; — FB; --- MIT; - - - Colombo et al. [28]

The radial distribution of the average bubble diameter for the DEBORA experiment, as shown in Figure 6, demonstrates that bubble size increases in moving away from the wall, reaching a peak value near the centre of the pipe. The mechanistic model provides the superior prediction of this overall trend but slightly under-predicts the bubble diameter near the pipe centre. This discrepancy is likely due to limitations in the model's treatment of bubble coalescence and interactions within the bulk flow, which would affect the predicted bubble size in the core region. Although both boiling model approaches use the same population balance, the MIT model exhibits a similar trend but predicts smaller bubble sizes compared to the mechanistic model and significantly under-predicts experimental data at the pipe centre. This discrepancy is likely due to the different void profiles between the two models which will affect coalescence and break-up differently. In contrast, the predictions from [28] significantly under-predict the bubble size across the bulk of the radial profile, with the exception of the peak at r/R ≈ 0.65. This under-prediction highlights the need for further development in the population balance model used in [28], which is coupled with the boiling model, to improve the accuracy of bubble size predictions. Notably, the average bubble diameter near the wall differs significantly between the various models, which reflects the initial bubble departure diameter when the bubbles first detach from the wall and move into the bulk of the flow. This variation in departure diameter can negatively affect the prediction of radial void fraction.

7. CONCLUSIONS

This study evaluated the performance of two boiling models, a mechanistic force balance approach and a reduced correlation-based MIT model, coupled with large eddy simulation for predicting turbulent subcooled flow boiling. Validated against data from the DEBORA [26] experiments and those of Bartolomei and Chanturiya [27], the mechanistic model demonstrated superior accuracy in predicting bubble dynamics due to its detailed treatment of heat transfer mechanisms. However, it required greater computational resources compared to the MIT model, which offered a more efficient but less precise alternative.

Although the RANS-based approach relies on an averaging methodology and does not fully resolve turbulence and phase interactions, it provides good predictions of certain parameters. However, RANS models tend to oversimplify the complex, unsteady nature of boiling flows, which reduces their accuracy in predicting key parameters. In contrast, LES offers a more physically realistic representation by resolving large turbulent structures while modelling only the smaller subgrid-scale eddies. This enhanced turbulence resolution improves the accuracy of predictions for bubble departure dynamics, void fraction distribution, and heat transfer mechanisms, particularly in regions dominated by strong phase interactions and subcooling effects. However, LES also exhibits some over-prediction, especially in terms of wall temperature, indicating the need for further refinement to enhance its predictive accuracy.

ACKNOWLEDGEMENTS

This work is supported by the Ministry of Higher Education and Scientific Research of Libya.

REFERENCES

[1] Dhir, V. K., 1998, "Boling Heat Transfer", *Annu. Rev. Fluid Mech.*, Vol. 30, pp. 365-401.

[2] Zhou, K., Coyle, C., Li, J., Buongiorno, J., and Li, W., 2017, "Flow Boiling in Vertical Narrow Microchannels of Different Surface Wettability Characteristics", *Int. J. Heat Mass Transf.*, Vol. 109, pp. 103-114.

[3] Fang, X., Yuan, Y., Xu, A., Tian, L., and Wu, Q., 2017, "Review of Correlations for Subcooled Flow Boiling Heat Transfer and Assessment of their Applicability to Water", *Fusion Eng. Des.*, Vol. 122, pp. 52-63.

[4] Colombo, M., and Fairweather, M., 2016, "Accuracy of Eulerian-Eulerian, Two-Fluid CFD Boiling Models of Subcooled Boiling Flows", *Int. J. Heat Mass Transfer*, Vol. 103, pp. 28-44.

[5] Prosperetti, A., and Tryggvason, G., 2007, "Computational Methods for Multiphase Flow", *Cambridge University Press*.

[6] Kurul, N., and Podowski, M.Z., 1990, "Multidimensional Effects in Forced Convection Subcooled Boiling", *Proc. 9th International Heat Transfer Conference*, Jerusalem, Israel, pp. 21-26.

[7] Tolubinsky, V.I., and Kostanchuk, D.M., 1970, "Vapor Bubbles Growth Rate and Heat Transfer Intensity at Subcooled Water Boiling", *Proc. 4th International Heat Transfer Conference*, Paris, France, B-2.8.

[8] Cheung, S.C.P., Vahaji, S., Yeoh, G.H., and Tu, J.Y., 2014. "Modeling Subcooled Flow Boiling in Vertical Channels at Low Pressures – Part 1: Assessment of Empirical Correlations", *Int. J. Heat Mass Transfer*, Vol. 75, pp. 736-753.

[9] Klausner, J. F., Mei, R., Bernhard, D. M., and Zeng, L. Z., 1993, "Vapor Bubble Departure in Forced Convection Boiling", *Int. J. Heat Mass Transf.*, Vol. 36, pp. 651-662.

[10] Sugrue, R., and Buongiorno, J., 2016. "A Modified Force-Balance Model for Prediction of Bubble Departure Diameter in Subcooled Flow Boiling", *Nucl. Eng. Des.*, Vol. 305, pp. 717-722.

[11] Yun, B.J., Splawski, A., Lo, S., and Song, C.H., 2012, "Prediction of a Subcooled Boiling Flow with Advanced Two-Phase Flow Models", *Nucl. Eng. Des*., Vol. 253, pp. 351-359

[12] Colombo, M., and Fairweather, M., 2015. "Prediction of Bubble Departure in Forced Convection Boiling: A Mechanistic Model", *Int. J. Heat Mass Transfer*, Vol. 85, pp. 135-146.

[13] Kommajosyula, R., 2020, "Development and Assessment of a Physics-Based Model for Subcooled Flow Boiling with Application to CFD", *PhD Thesis, Massachusetts Institute of Technology*.

[14] Pham, M., Bois, G., Francois, F., and Baglietto, E., 2023. "Assessment of State-of-the-art Multiphase CFD Modeling for Subcooled Flow Boiling in Reactor Applications", *Nucl. Eng. Des*., Vol. 411, 112379.

[15] Owoeye, E.J., Schubring, D., 2016. "CFD Analysis of Bubble Microlayer and Growth in Subcooled Flow Boiling", *Nucl. Eng. Des.*, Vol. 304, pp. 151-165.

[16] Sato, Y., Sadatomi, M., and Sekoguchi, K., 1981, "Momentum and Heat Transfer in Two-Phase Bubble Flow – I. Theory", *Int. J. Multiph. Flow*, Vol. 7, pp. 167-177.

[17] Germano, M., Piomelli, U., Moin, P., and Cabot, W.H., 1991, "A Dynamic Subgrid-Scale Eddy Viscosity Model", *Phys. Fluids*, Vol. 3, pp. 1760-1765.

[18] Tomiyama, A., Kataoka, I., Zun, I., and Sakaguchi, T., 1998, "Drag Coefficients of Single Bubbles Under Normal and Micro Gravity Conditions". *JSME Int. J. Ser. B*, Vol. 41, pp. 472-479.

[19] Lopez de Bertodano, M., 1998, "Two Fluid Model for Two-Phase Turbulent Jet", *Nucl. Eng. Des.*, Vol. 179, pp. 65-74.

[20] Prince, M.J., and Blanch, H.W., 1990, "Bubble Coalescence and Break-up in Air-sparged Bubble Columns", *AIChE J*, Vol. 36, pp. 1485-1499.

[21] Lehr, F., Millies, M., and Mewes, D., 2002, "Bubble-size Distributions and Flow Fields in Bubble Columns", *AIChE J*, Vol. 48, pp. 2426-2443.

[22] Hibiki, T., and Ishii, M., 2003, "Active Nucleation Site Density in Boiling Systems", *Int. J. Heat Mass Transfer*, Vol. 46, pp. 2587-2601.

[23] Cole, R., 1960, "A Photographic Study of Pool Boiling in the Region of the Critical Heat Flux", *AIChE J.*, Vol. 6, pp. 533-538.

[24] Lemmert, M., Chawla, J.M., 1977, "Influence of flow velocity on surface boiling heat transfer coefficient", in: E. Hahne, U. Grigull (Eds.), *Heat Transfer in Boiling, Academic Press and Hemisphere*, New York, pp. 237–247.

[25] Spalding, D. B., 1961, "A Single Formula for the Law of the Wall", *J. Appl. Mech. Trans. ASME*, Vol. 28, pp. 455-458.

[26] Garnier, G., Manon, E., and Cubizolles, G., 2001, "Local Measurements of Flow Boiling of Refrigerant 12 in a Vertical Tube", *Multiph. Sci. Technol.*, Vol. 13, pp. 1-111.

[27] Bartolomei, G.G., and Chanturiya, V.M., 1967, "Experimental Study of True Void Fraction when Boiling Subcooled Water in Vertical Tubes", *Therm. Eng*., Vol. 14, pp. 123-128.

[28] Colombo, M., Thakrar, R., Fairweather, M., and Walker, S.P., 2019, "Assessment of Semi-Mechanistic Bubble Departure Diameter Modelling for the CFD Simulation of Boiling Flows", *Nucl. Eng. Des.*, Vol. 344, 15-27.